

Electronic Excitations Generated by the Deposition of Mg on Mg Films

U. Hagemann, D. Krix, and H. Nienhaus*

*Faculty of Physics, University of Duisburg-Essen and Center for NanoIntegration (CeNIDE),
Lotharstrasse 1, 47048 Duisburg, Germany*

(Received 8 July 2009; published 14 January 2010)

Nonadiabatic processes are observed during growth of Mg atoms from the gas phase on Mg films. Chemicurrents are measured in thin film Mg/*p*-Si(001) Schottky diodes which are exposed to thermally evaporated Mg atoms. The photonic and chemical contributions to the observed reverse currents in the devices can be distinguished by varying the Mg atom flux and by independent measurements using an empty evaporator as a source of heat radiation.

DOI: 10.1103/PhysRevLett.104.028301

PACS numbers: 82.20.Gk, 68.43.-h, 79.20.Rf

When metal atoms from the gas phase are deposited on a metal surface the initially localized valence electrons of the atom are transferred into the delocalized states of the solid metal. This condensation is an exothermic process. Its released energy can be deduced from the heat of vaporization or sublimation which are typically a few eV/atom [1,2]. Although much effort has been spent on the detailed study of the nonmetal-metal transition [3,4], much less is known about the dynamics and the mechanisms of how the condensation energy is dissipated. This issue is important not only for the understanding of the elementary steps of metallization but also for describing the metal film growth. The present study addresses this issue and, in particular, the nonadiabatic energy transfer during the growth of metal films under ultrahigh vacuum conditions.

Since the detection of chemically induced electronic excitations has become feasible by the use of thin-film electronic devices, nonadiabatic dissipation of chemical energy during gas-surface reactions has gained much attention [5–10]. In addition, progress in the theory of nonadiabatic processes at surfaces, e.g., applying time-dependent density functional theory (TD-DFT) or electronic friction models has improved the understanding of the elementary steps behind the excitation mechanism [11–14]. Obviously, electronic excitation with mobile hot charge carriers is a common feature of exothermic metal surface reactions in which bonds are formed. So far, for a variety of gas-surface and heterogeneous catalytic reactions the nonadiabatic character of energy dissipation was successfully demonstrated applying exoemission experiments [15–19] or using the chemicurrent scheme [5–10,20–23].

The present study investigates the energy transfer during the growth of Mg on Mg. From the temperature dependence of the vapor pressure the condensation energy is expected to be approximately 1.5 eV [2,24]. As an alkali earth metal, Magnesium has a closed electronic shell and metallization occurs by hybridization of *s*- and *p* orbitals while approaching the surface corresponding to a Wilson-type transition [4,25]. A chemicurrent setup has been used to find out if the rapid rearrangement of the electronic

structure and the release of the condensation energy generate electronic excitations. Chemicurrent measurements were performed with Mg/*p*-Si(001) Schottky diodes which were fabricated by depositing Mg on clean and hydrogen-passivated Si(001) surfaces ($\rho = 1\text{--}10 \Omega \text{ cm}$) at a temperature of 120 K. Mg atoms were evaporated from a vitreous carbon (VC) crucible of a commercial effusion cell (Createc) under ultrahigh vacuum conditions with a base pressure below 10^{-9} hPa. The diode area was approximately 0.75 cm^2 and the metal film thickness varied between 2 and 40 nm. After deposition the diodes were annealed to room temperature to improve the metal film quality. From *in situ* current-voltage measurements a homogeneous Schottky barrier height of 0.5 ± 0.1 eV was determined. This value indicates that no intermixing of Mg and Si occurs since Mg silicides lead to larger barrier heights on *p*-Si [26]. The Schottky diode was placed in front of a thermal Mg evaporator equipped with a beam shutter. The reverse current response in the device was monitored under zero bias and at low diode temperatures of typically 120 K. In the upper panel of Fig. 1, the principle of the current generation and detection is schematically presented. The scheme shows an energy-space diagram and the bending of the silicon band edges (VBM, CBM) resulting in the Schottky barrier Φ_B . Since the thermal evaporator is also a heat radiator, three different processes can create a reverse current in the diode. Process (1) demonstrates the chemicurrent mechanism which generates electron-hole pairs at the surface due to nonadiabatic energy dissipation. Hot holes are detected in the device after ballistic transport through the metal film and transmission across the Schottky barrier. Internal photoemission (2) may occur from photons with energies above Φ_B and the photoeffect (3) is due to effective absorption of photons with energies above the fundamental band gap E_{gap} in the space charge layer. Mg is sublimated at low evaporator temperatures typically between 570 and 620 K and, hence, photonic effects are small enough to allow chemicurrent detection in the pA range.

The lower panel of Fig. 1 shows a current detected in a 5 nm-Mg/*p*-Si(001) diode placed in front of the Mg

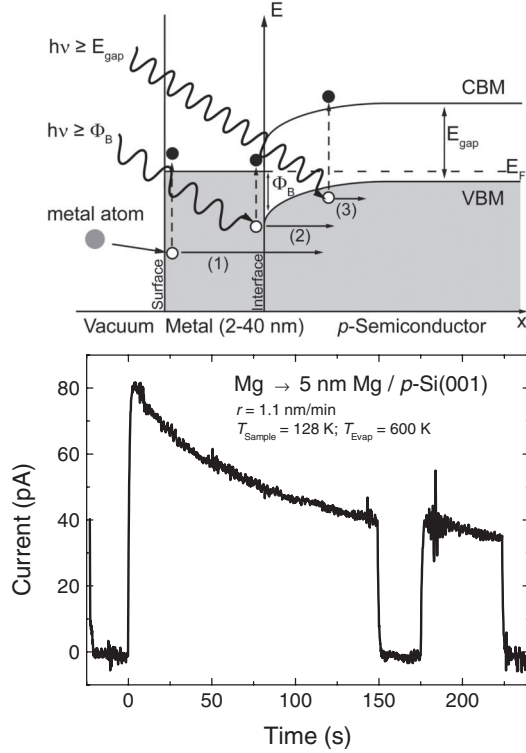


FIG. 1. Upper panel: Energy-space diagram of a thin-film metal-semiconductor diode. Three processes can generate a reverse current in the device upon exposing the diode to Mg atoms from a thermal evaporator: (1) chemicurrent, (2) internal photoemission and (3) photoeffect. Lower panel: Current trace detected from a 5 nm Mg/*p*-Si(001) diode upon exposure of Mg atoms.

evaporator which is held at $T_{\text{Evap}} = 600$ K. The Mg deposition rate was determined with a commercial calibrated quartz microbalance (Inficon, 6 MHz quartz crystals) as 1.1 nm/min ($\pm 0.5\%$) which corresponds to an impinging rate of 6×10^{13} atoms/s onto the diode. When the shutter is closed the background current is zero within the noise level of 2 pA. At $t = 0$, the shutter is opened and an instantaneous current response of 80 pA is observed. The current decreases exponentially due to the growing Mg film. After 150 s the shutter is closed for 25 s. The exponential attenuation of the current is resumed after reopening the shutter. The attenuation length λ is determined as 5.4 nm from the exponential decay, i.e., $\exp(-rt/\lambda)$ where r denotes the growth rate. This value is close to what was reported earlier for chemicurrents [27]. As demonstrated below, attenuation of infrared light leads to much larger λ values. This is a first indication that the observed current is predominantly due to hot charge carrier creation at the surface. Thermoelectric effects can be completely neglected. They cannot explain the decay as well as the magnitude of the current. If every atom deposits 1.5 eV the total power is 36 μ W. Assuming a stationary heat flow through the diode the temperature difference across the 0.6 mm thick Si wafer can be calculated with the thermal

conductance of Si [28] as 0.6 μ K which results in a thermoelectric power of 3 nV. However, this voltage cannot induce a measurable current as for the Schottky diodes contact resistances at zero bias are measured in the $G\Omega$ range.

To eliminate the effect of attenuation of the current by the Mg film growth, the opening of the shutter was reduced to a few seconds and the respective currents were recorded for varying Mg atom fluxes adjusted by the evaporator temperature. Response current spikes for Mg/*p*-Si(001) diodes with initial film thicknesses of 3 and 6 nm are plotted as a function of time and evaporator temperature in Fig. 2. Decreasing the evaporator temperature leads to a significant reduction of the reverse current in the device due to a lower Mg atom flux and reduced thermal radiation from the evaporator. In addition, the diode with the larger metal film thickness is much less sensitive in agreement with the observation in Fig. 1. The measured current comprises three additive contributions according to the above introduced three processes of current generation, i.e.,

$$I = I_{CC} + I_{IPE} + I_P \\ \approx \alpha \exp\left(-\frac{H_{\text{sub}}}{k_B T_{\text{evap}}}\right) + \beta \exp\left(-\frac{\Phi_B}{k_B T_{\text{evap}}}\right) \\ + \gamma \exp\left(-\frac{E_{\text{gap}}}{k_B T_{\text{evap}}}\right).$$

The first term represents the contribution of the chemicurrent with efficiency α and H_{sub} as the enthalpy of sublimation of Mg. The second and third term describe the

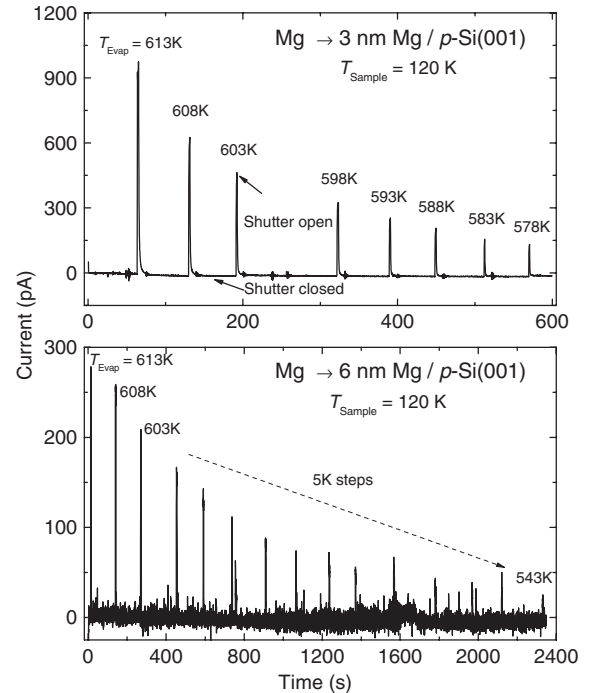


FIG. 2. Reverse current spikes detected from two Mg/*p*-Si Schottky diodes with different initial Mg film thicknesses upon exposure to an atomic Mg beam.

internal photoemission (I_{IPE}) and the photoeffect (I_p). They are derived from Wien's law which is valid in this present case of low evaporator temperatures and large barrier energies. The maximum of the Planck's radiation curve is found at a photon energy of 0.15 eV for $T_{\text{Evap}} = 620$ K which is much smaller than the barrier height (0.5 eV) or the band gap energy (1.16 eV). The coefficients β and γ include the photon mode density and the solid angle between sample and evaporator. They have a negligible temperature dependence due to the integration of the radiation curve for photon energies above Φ_B and E_{gap} , respectively.

To distinguish the different contributions the current values are plotted as a function of the evaporator temperature in an Arrhenius diagram as shown in Fig. 3. In the lower panel of the figure the Mg deposition rate as determined with the quartz microbalance is displayed. From the slope the enthalpy of sublimation of Mg is measured as $H_{\text{sub}} = 1.3$ eV for our experiments. This value is slightly

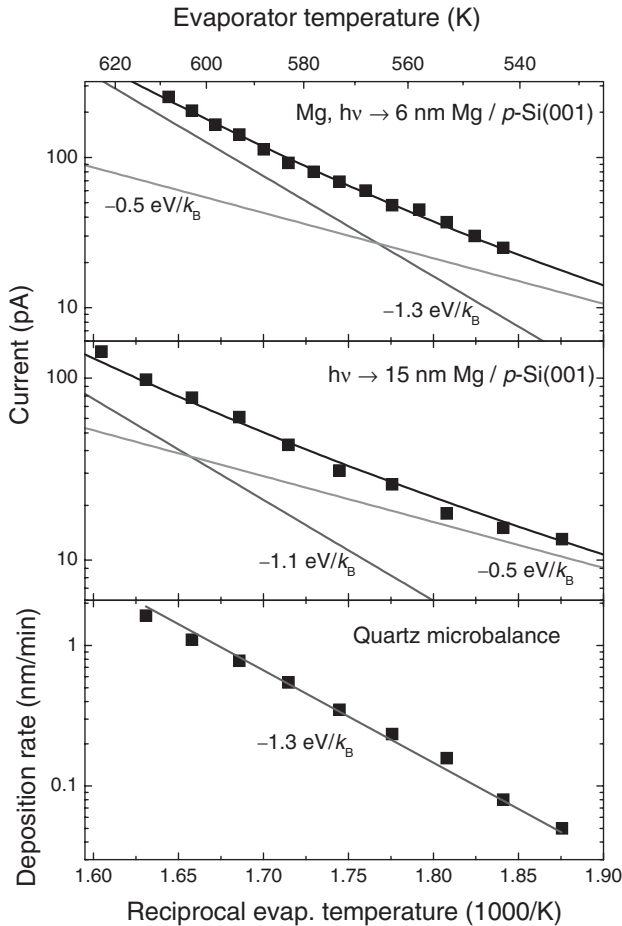


FIG. 3. Arrhenius plots of detected currents in the diode and of the deposition rate. The numbers represent the slopes of the exponential functions. Top panel: current detected from a diode exposed to an atomic Mg beam from the thermal evaporator. Middle panel: current detected from a diode exposed to radiation only. Lower panel: deposition rate yielding the enthalpy of sublimation.

smaller than literature data of 1.5 eV [2,24]. The top panel of Fig. 3 represents the current data detected at the 6 nm Mg/Si diode as shown in Fig. 2. The solid line is a fit which consists of the sum of two exponentials with energies according to chemicurrent (1.3 eV) at large and internal photoemission current (0.5 eV) at low evaporator temperatures. The photocurrent is too small to be resolved on the dominating chemicurrent background. Pure photoinduced currents are presented in the middle panel in Fig. 3 where the Mg/*p*-Si(001) diode is exclusively exposed to the heat radiation of an equally constructed but empty evaporator. Here, two exponentials are observed which can be attributed to internal photoemission (0.5 eV) and to the photoeffect (1.1 eV). Therefore, as soon as Mg is deposited onto the diode the chemicurrent exceeds the photocurrent at large evaporation temperatures but the internal photoemission current can still be observed at low temperatures due to a vanishing deposition rate. Taking the difference of the currents in the same sample when facing the Mg and the empty evaporator, respectively, is not practical as the emissivities of the two evaporators are different.

Data as shown in Fig. 3 were collected for many Mg/*p*-Si diodes with different initial Mg film thicknesses. The respective energies of the fitting exponentials are summarized in Fig. 4. The diagram gives strong evidence that independent of the film thickness chemicurrents, i.e., nonadiabatically excited charge carriers are observed at large evaporator temperatures. The energy in the exponential yields the enthalpy of sublimation of Mg, i.e., 1.3 eV (solid rectangles). For low evaporator temperatures, a value close to the Schottky barrier height is found due to internal photoemission (solid circles). In addition, the current data of diodes are included in Fig. 4 which were only irradiated with photons due to heat radiation from an empty evaporator (open symbols). Here, an energy of 1.03 ± 0.07 eV is extracted for the fitting exponential at higher evaporator temperatures. It is significantly smaller than the enthalpy of sublimation. The deviation from the band gap energy (1.16 eV) can be explained by the indirect light absorption process in Si which needs a phonon for band-to-band transitions. Hence, the fundamental absorption starts at energies below E_{gap} [29].

Since the currents were measured with diodes of different initial film thicknesses the attenuation lengths can be determined. For chemicurrents, a value of $\lambda = 4.3 \pm 1.0$ nm is found which is in agreement with the value from Fig. 1. The experiments with pure heat radiation yield an attenuation length for the photocurrent of 21 ± 4.0 nm which is larger than values calculated from optical data of Mg. From the extinction coefficient, the penetration depths of photons in bulk Mg are calculated as 14 nm for $h\nu = 0.5$ eV and 8 nm for $h\nu = 1.16$ eV [30]. The difference to the measured 21 nm can be explained by the laterally varying Mg film thickness. Nonuniform film growth leads to larger attenuation lengths since the semiconductor surface is partly covered with a metal film thinner than the

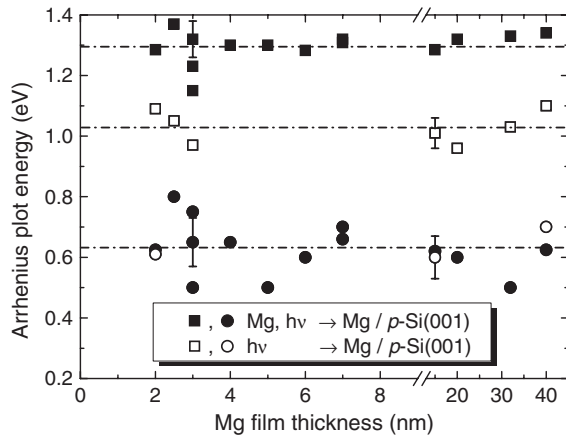


FIG. 4. Energies extracted from fitting exponentials of various Arrhenius plots for Mg/Si Schottky diodes with different initial Mg film thicknesses. The solid symbols represent data from diodes which were exposed to thermally evaporated Mg atoms. Open symbols give data from irradiated diodes. The energy at 1.3 eV corresponds to the enthalpy of sublimation (chemicurrent), at 1.03 eV to the indirect band-to-band absorption energy (photocurrent) and at 0.6 eV to the Schottky barrier height (internal photoemission).

nominal coverage. The presented results demonstrate that the observed currents in the Mg/*p*-Si(001) Schottky diodes which are exposed to an atomic Mg beam are predominantly generated by electronic excitation of the metal electrons during metal film growth. The efficiency can be determined from the deposition rate and the measured currents in Fig. 2. For the 3 nm Mg/Si diode a chemicurrent of 340 pA is measured for a deposition rate of 6×10^{13} atoms/s onto the device area (0.75 cm^2) at 598 K, yielding an efficiency of 3.5×10^{-5} elementary charge/atom. This value is by a factor of 1000 smaller than for chemicurrents during oxidation of Mg by O_2 [9]. From this value it cannot be determined how much energy is dissipated nonadiabatically into electron-hole pairs and how much is dissipated directly into the phonon system because the diode does not detect excited charge carriers with energies below the Schottky barrier. However, the significant chemicurrent implies the surprising result that metal-on-metal growth occurs with nonadiabatic energy dissipation at all. Since no charge transfer processes are expected, the excitation mechanism is likely to be electronic friction [11,13]. In case of Mg deposition, hybridization of $3s$ - and $3p$ -levels must happen to understand the metallic character of the Mg solid [4]. This may happen by exchange between atomic and metal electrons causing a strong interaction which may be the driving force for electronic excitations.

In conclusion, chemicurrents were detected during Mg deposition on Mg/*p*-Si(001) Schottky diodes with varying metal film thicknesses demonstrating that nonadiabatic energy dissipation occurs during metal condensation. The Mg atom was produced by thermal evaporation and the chemicurrent efficiency was found to be in the 10^{-5}

elementary charge/atom range. Photocurrents and internal photoemission currents in the devices could be distinguished from the chemicurrent contribution by varying the evaporator's temperature and by measuring the photonic effect by use of an empty evaporator independently. The chemicurrent is exponentially attenuated with increasing Mg film thickness. The attenuation length is determined as approximately 5 nm which is typical for hot charge carrier transport in metal films. The results give rise to a new view on the dynamics of metal film growth and metal-on-metal interactions in general as most of the homoepitaxial systems have a much higher exothermicity than in case of Mg.

The financial support by the Deutsche Forschungsgemeinschaft (DFG-SFB616) is gratefully acknowledged.

*hermann.nienhaus@uni-due.de

- [1] *Smithells Metals Reference Book*, edited by W.F. Gale (Elsevier, Amsterdam, 2004), 8th ed.
- [2] C.B. Alcock *et al.*, *Can. Metall. Q.* **23**, 309 (1984).
- [3] E.W. Plummer and P.A. Dowben, *Prog. Surf. Sci.* **42**, 201 (1993).
- [4] P.A. Dowben, *Surf. Sci. Rep.* **40**, 151 (2000).
- [5] H. Nienhaus *et al.*, *Phys. Rev. Lett.* **82**, 446 (1999).
- [6] B. Gergen *et al.*, *Science* **294**, 2521 (2001).
- [7] H. Nienhaus, *Surf. Sci. Rep.* **45**, 1 (2002).
- [8] B. Roldan-Cuenya *et al.*, *Phys. Rev. B* **70**, 115322 (2004).
- [9] S. Glass and H. Nienhaus, *Phys. Rev. Lett.* **93**, 168302 (2004).
- [10] D. Krix *et al.*, *Phys. Rev. B* **75**, 073410 (2007).
- [11] D.M. Bird, *Surf. Sci.* **602**, 1212 (2008).
- [12] M.S. Mizielinski *et al.*, *J. Chem. Phys.* **126**, 034705 (2007).
- [13] J.R. Trail *et al.*, *Phys. Rev. Lett.* **88**, 166802 (2002).
- [14] M. Lindenblatt and E. Pehlke, *Phys. Rev. Lett.* **97**, 216101 (2006).
- [15] T. Greber, *Surf. Sci. Rep.* **28**, 1 (1997).
- [16] L. Hellberg *et al.*, *Phys. Rev. Lett.* **74**, 4742 (1995).
- [17] A. Bottcher *et al.*, *Surf. Sci.* **280**, 170 (1993); *Phys. Rev. Lett.* **65**, 2035 (1990).
- [18] G.C. Allen *et al.*, *Surf. Sci.* **102**, 207 (1981).
- [19] B. Kasemo, *Solid State Commun.* **15**, 571 (1974).
- [20] B. Gergen *et al.*, *Surf. Sci.* **488**, 123 (2001).
- [21] B. Mildner *et al.*, *Chem. Phys. Lett.* **432**, 133 (2006).
- [22] E.G. Karpov and I.I. Nedrygallov, *Appl. Phys. Lett.* **94**, 214101 (2009).
- [23] Y.J. Park *et al.*, *Nano Lett.* **8**, 2388 (2008).
- [24] W.P. Gilbreath, Report No. NASA-TN-D-2723, 1965.
- [25] I.N. Yakovkin, *Surf. Sci.* **406**, 57 (1998).
- [26] H. Nienhaus *et al.*, *J. Vac. Sci. Technol. A* **25**, 950 (2007).
- [27] H. Nienhaus *et al.*, *Surf. Sci.* **514**, 172 (2002).
- [28] *Semiconductors: Data Handbook*, edited by O. Madelung (Springer, Berlin, 2004), 3rd ed.
- [29] P.Y. Yu and M. Cardona, *Fundamentals of Semiconductors* (Springer, Berlin, 2001), 3rd ed., p. 274.
- [30] *Handbook of Optical Constants of Solids*, edited by E.D. Palik (Academic Press, Orlando, 1985).